参赛队员姓名：Yuehan Wang

中学：Oaks Christian School

省份：California

国家：United States of America

指导教师姓名：Prof. Jian Lin, Prof. Lin Li

论文题目：Total Removal of Formaldehyde indoor by Al-based Metal-Organic Framework Decorated with Pt Nanoclusters via Tandem Adsorption and Catalysis

Total Removal of Formaldehyde indoor by Al-based Metal-Organic Framework Decorated with Pt Nanoclusters via Tandem Adsorption and Catalysis

Shing-Tung Yau High School Science Award for Chemistry 2020

Name: Yuehan Wang

School: Oaks Christian School

ABSTRACT

In terms of the elimination for indoor HCHO pollutant, good removal efficiency and long lifetime at ambient conditions are desirable. Herein, a bifunctional, low-cost catalyst of Pt/CAU-1-$(OH)_2$ is fabricated with Pt loading of only 0.1 wt%, possessing good ability of adsorption and catalysis for HCHO. Metal-organic framework (MOF) materials of the established CAU type are synthesized and utilized as HCHO adsorbents. The long-lasting efficacy and remarkable adsorption capacities for HCHO are obtained, of 1.6 mmol g_{cat}^{-1} on CAU-1-$(OH)_2$ and 3.2 mmol g_{cat}^{-1} on CAU-1-NH_2, which are considerably higher than those for previously reported adsorbents. This benefits from large surface area, sufficient porosity, and Lewis basic functional groups (-NH_2 and -OH) of these MOFs. Following the facile dispersion of ~1 nm Pt clusters on the CAU-1-$(OH)_2$ MOF, the adsorbed HCHO pollutant is efficiently oxidized to CO_2 and water, achieving complete elimination of HCHO at ambient conditions. Moreover, the catalyst of 0.1Pt/CAU-1-$(OH)_2$ shows a good stability for prolonged HCHO oxidation. Consequently, it can be concluded that this method of combining adsorption and catalysis is an effective one for total elimination of HCHO at ambient conditions.

Key words: Adsorption, Oxidation, Pt, HCHO, Metal-organic framework

ABBREVIATION

MOF	Metal-Organic Framework
CAU	Christian-Albrechts-University
SBS	Sick-Building-Syndrome
ppm	Parts Per Million
VOC	Volatile Organic Compound
MEK	Methyl Ethyl Ketone
PCE	Tetrachloroethylene
XRD	X-ray Diffraction
SEM	Scanning Electron Microscope
TGA	Thermogravimetric Analysis
XPS	X-ray Photoelectron Spectroscopy
HAADF-STEM	High-Angular Dark-Field Scanning Transmission Electron Microscopy
ICP-AES	Inductively Coupled Plasma-Atomic Emission Spectrometry
EG	Ethylene Glycol
RH	Relative Humidity
WHSV	Weight Hour Space Velocity

CONTENTS

1. INTRODUCTION

1.1 Sources and hazards of formaldehyde

Formaldehyde (HCHO), a significant air pollutant indoor, is a flammable, colorless and strong-smelling chemical. It is emitted from urea resin that is widely used in decorative furniture and construction materials, such as the insulating material for housing and public buildings, furniture coatings, pressed-wood products and adhesives. Long time exposure of HCHO can cause sick-building-syndrome (SBS), such as skin allergies, throat and nasal irritation, leukemia and cancers[1]. Therefore, it is imperative to be able to eliminate HCHO at ambient temperature and humidity.

1.2 Methods of HCHO elimination

Currently, various strategies including adsorption of physical and chemical process, photocatalysis, and thermal catalytic decomposition, have been developed to lower concentration of formaldehyde, or remove it to a sufficient extent that it can satisfy human needs and stringent environmental regulations currently recommended[2]. In terms of adsorption method, the common adsorbents mainly contain the porous materials (activated carbon) and stratified material. The properties of high surface area, small pore size and high microporous volume have been found to faciliate the physical adsorption of HCHO[3]. Furthermore, presence of Lewis basic functional groups (hydroxyls, amino and sulfure et al.) in adsorbents can also enhance the chemical adsorption affinity of the material for HCHO[4]. However, although the adsorption method for removing HCHO pollutants is easily performed, limited capacities of adsorption and the difficulty of regeneration hinder its practical application. By photocatalytic oxidation technologies, the removal efficiency for HCHO has

been improved. However, the generated toxic by-products can cause secondary pollution, and an additional illumination apparatus is required, resulting in higher operating cost for its use and more severe reaction conditions[5]. Catalytic oxidation method, utilizing the oxygen present in air to transform the HCHO into the non-toxic carbon dioxide and water, is regarded as the most promising approach to eliminate HCHO due to the advantages of remarkable efficiency, low energy requirements and environmental-friendliness. The catalysts deployed mainly contain either transition metal oxides (MnO_2, CeO_2, Co_3O_4, etc.), composite metal oxide (Fe_2O_3-SiO_2, MnO_2-C_3O_4-CeO_2, CuO-MnO_2, etc.) or supported noble metals (Pt, Rh, Au, Ag etc.)[6]. Pt-based catalysts is considered as the benchmark system in HCHO oxidation at low temperature. For example, on the catalysts containing Pt/TiO_2, with Na^+ as a promotor, the HCHO was entirely converted to CO_2 and H_2O at ambient conditions[7]. Nevertheless, in a practical environment, HCHO concentration is of an extremely low level (< 1 ppm) and the release period may last as long as ten years. Thus, developing a catalyst endowing a high removal efficiency and long lifetime is highly desirable for the thorough elimination of HCHO.

1.3 HCHO removal by adsorption and catalysis

The hybrid technology combining adsorption and catalysis processes is a proven method for the removal of low-concentration VOC (Volatile Organic Compound) pollutants, where the two processes can complement one another cost effectively. The conventional adsorption/oxidation instrument is reported in the elimination of Methyl Ethyl Ketone (MEK) and Tetrachloroethylene (PCE)[8], as presented in the scheme of Figure 1a. The porous zeolite molecular sieve (HFAU) as the adsorbent is put in the upper layer while a supported platinum catalyst is in the lower layer for catalytic oxidation at elevated temperature. The challenges

involving complicated operation and high cost are brought about due to the coexistence of adsorption and oxidation as separate processes in this scheme. Subsequently, a bifunctional technology based on an Ag-MnO_x-CeO_2 catalyst was developed. As shown in Figure 1b, HCHO was stored as formate at room temperature; once saturation was reached, the catalyst was heated to a high temperature of 290 °C during which the stored formate species were completely decomposed, resulting in the regeneration of catalyst[9]. The same research group subsequently developed a CoMn catalyst with a three-dimensional ordered cubic mesoporous structure which could catalyze this process[10]. The catalyst exhibited a higher storage capacity for HCHO and a better catalytic performance, as the stored HCHO could be completely oxidized at 135 °C. However, this process still requires a relatively high temperature to regenerate, making operation complexity and high energy consumption.

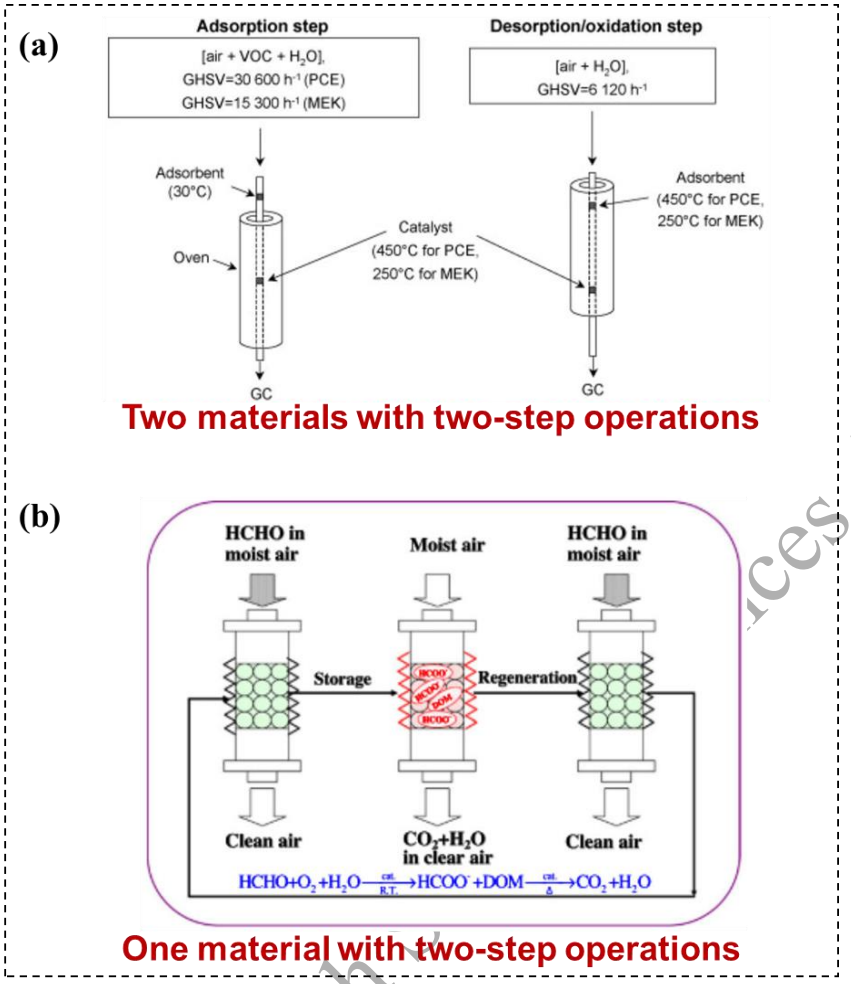

Figure 1. (a) Scheme of adsorption/oxidation apparatus for conventional VOCs removal and (b) cycling process for HCHO "storage-oxidation".

1.4 The target of this research

Even though an effective method for HCHO elimination has been achieved by the combination of adsorption and catalysis, the multi-step operation and high conversion temperature endowed drawbacks of catalyst regeneration and high energy consumption. So far, a material has not been developed that can store HCHO by adsorption and then catalyze oxidation to the non-toxic CO_2 and H_2O at ambient conditions. Therefore, it is a formidable but meaningful challenge to exploit a catalyst that can integrate high adsorption capacities and outstanding oxidation efficiency into a one-step process. As is well known, porous materials

such as carbon, zeolite are good candidates as adsorbents and supports to stabilize the noble metal particles. The metal-organic frameworks (MOFs) with porous crystalline may constitute the ideal support. High surface areas and pore volumes are favorable for their usage in adsorption and gas storage. Furthermore, their flexible frameworks can provide the abundance of potential coordination sites, defects and porosities that are required for anchoring noble metal catalysts[11]. Perhaps most importantly, MOF materials are easily modified with various functional groups, according to the particular application.

Among the diverse MOFs that have been synthesized thus far, the Al-containing compounds of the CAU type have been widely deployed in gas storage, as their property can be adjusted in detail for specific applications. For instance, a CAU MOF decorated with hydrophobic groups has been employed to adsorb trace toluene to enable indoor air purification, which possesses a much higher adsorption capacity compared to conventional adsorbents as zeolites ZSM-5 and 13X[12]. Si et al. utilized the amine-decorated microporous CAU-1-NH_2 material for CO_2 adsorption and separation[13]. High CO_2 uptake capacity was obtained by binding with the Lewis basic groups. Although the CAU materials exhibit good performance in gas storage, application of CAU materials in catalysis has not yet been exploited. In this work, two kinds of CAU-1 materials are employed as HCHO adsorbents, which are respectively functionalized with NH_2 and OH groups. For achieving the tandem purification of HCHO by adsorption and oxidation, CAU-1-$(OH)_2$ is taken as a support to stabilize and disperse Pt nanoclusters, with a significantly lowered Pt loading (0.1 wt%). The structures of the CAU-1 and Pt/CAU-1 materials are reflected by various methods of X-ray diffraction (XRD), scanning electron microscopy (SEM), scanning transmission electron microscopy

(STEM), N_2 adsorption isotherms, thermogravimetric analysis (TGA), and X-ray photoelectron spectroscopy (XPS). Conducting adsorption and catalysis studies of HCHO with these materials is expected to lead to significantly superior results as compared to previously published materials.

2. EXPERIMENTAL SECTION

2.1 Preparation of catalysts

2.1.1 Chemicals

The reagents of 2,5-dihydroxyterephthalic acid ($H_2BDC\text{-}(OH)_2$, ≥99.99%) and 2-amino terephthalic acid ($H_2BDC\text{-}NH_2$, ≥99.99%) were purchased from TCI (Shanghai) Development Co., Ltd. Aluminum chloride ($AlCl_3 \cdot 6H_2O$, ≥99.99%), methanol (CH_3OH, ≥98.0%) and sodium hydroxide (NaOH, ≥98.0%) were produced by Kermel Chemical Reagent Company; $H_2PtCl_6 \cdot 6H_2O$ from Tianjin Feng Chuan Chemical Reagent Company. No further treatment was conducted before utilization.

2.1.2 Preparation of CAU-1 materials

Pure-phase CAU-1-$(OH)_2$ and CAU-1-NH_2 were synthesized using a common solvothermal method[14]. Taking the preparation of CAU-1-$(OH)_2$ as an example, 10.4 g $AlCl_3 \cdot 6H_2O$, 2.97 g $H_2BDC\text{-}(OH)_2$ were added in a breaker with 100 mL methanol in turn. Then 2 mol L^{-1} methanolic NaOH (4.5 mL, 9 mmol) solution was put in the above mixture. After stirring for 30 mins, the transparent yellow solution was obtained and then transferred into a teflon reactor. The reactor was placed into an 125 °C oven for 5 h with cooling naturally afterwards. To remove NaCl, the resulted suspension was separated by centrifugation and washed by methanol and ultrapure water in turn. The wet solid was transferred in a vaccum

oven at 60 °C. After around 12 h, a yellow microcrystalline solid was acquired. It is similar for preparing CAU-1-NH_2, where the starting material was replaced by H_2BDC-NH_2.

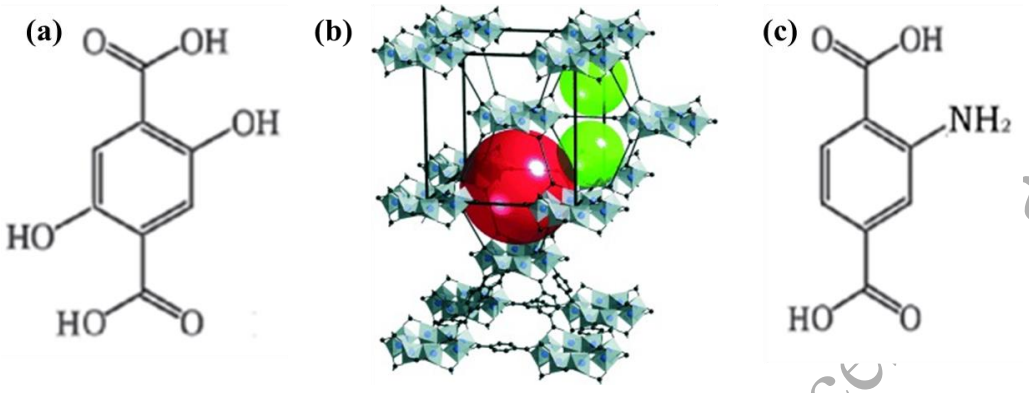

Figure 2. Structural diagrams of (a) H_2BDC-$(OH)_2$, (b) CAU-1-NH_2 (The spheres of red and green represent the distorted octahedral and tetrahedral cages, respectively) and (c) H_2BDC-NH_2[14].

2.1.3 Preparation of Pt cluster colloid

The colloid of Pt nanoclusters was synthesized by a reduction of a platinum precursor using alkaline ethylene glycol (EG), according to an established literature procedure[15]. 0.1 g NaOH was dissolved in 100 mL EG in a three-necked flask. Then it inputed 0.1 g of $H_2PtCl_6 \cdot 6H_2O$, which was stirred for around 30 mins to ensure good mixing at room temperature. Then the flask was moved to a oil-bath where the temperature was at 160 °C and then stirred for 3 h under argon atmosphere. As shown in Figure 3, a dark-brown colloid of Pt nanoclusters was obtained, denoted as Pt-NC.

Figure 3. The as-synthesized Pt-NC colloid.

2.1.4 Preparation of Pt/CAU-1 and Pt/Al_2O_3 catalyst

The convention method, excessive impregnation, was used to synthesize the sample of Pt/CAU-1. The CAU-1-$(OH)_2$ powder was dispersed in 100 mL EG under vigorous stirring at 80 ^oC. Take an appropriate amount of Pt clusters, and add them dropwise to the solution, as shown in Figure 4. It was stirred and standing for 3 h and 1 h, respectively. The obtained precipitate was treated via filtration and washing for 10 times to remove Cl ion. The resulted wet cake was transferred to an oven at 80 ^oC and then, dried for 12 h. The as-synthesized catalyst was denoted as nPt/CAU-1-$(OH)_2$, in which n was Pt loading.

For comparison, Pt/Al_2O_3 catalyst was also synthesized by the excessive impregnation method. The appropriate amount of Pt nanoclusters was added dropwise into an Al_2O_3/EG suspension in the water-bath of 80 ^oC. The suspension was treated as that of nPt/CAU-1-$(OH)_2$ with the as-synthesized catalyst denoted as nPt/Al_2O_3.

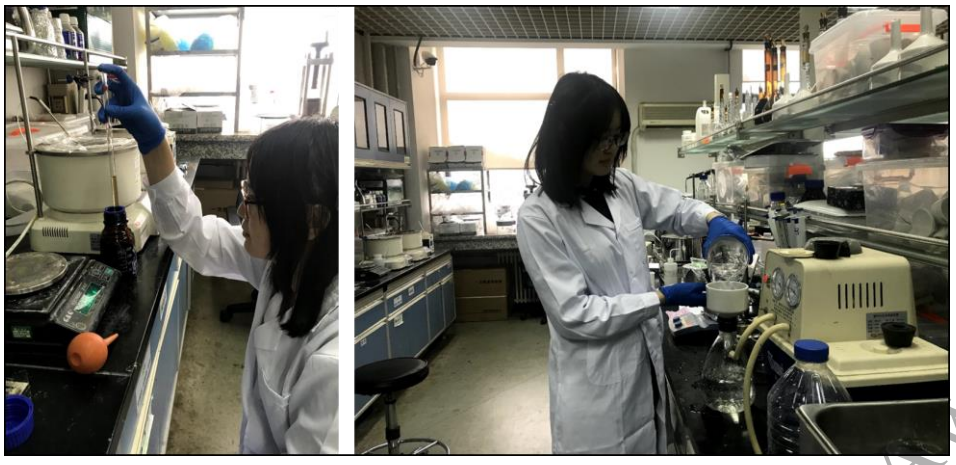

Figure 4. Synthesis of the Pt/CAU-1-$(OH)_2$ catalyst.

2.2 Characterizations

The structure of the CAU MOFs was confirmed using X-ray powder diffraction (XRD) technique with a PW3040/60 X'Pert PRO diffractometer with Cu Kα radiation (λ = 0.15432 nm, 40 kV, 40 mA) at a scan step of 10° min^{-1}. The experiment of nitrogen sorption was conducted on Micromeritics ASAP 2010 apparatus. The pore size distributions and specific surface area was evaluated according to BET surface models. The thermal stability was measured by thermal gravimetric analysis (TGA) using a Perkin-Elmer analyzer, in which the temperature of sample rose from 22 to 900 °C in argon atmosphere. For Pt/CAU-1, the Pt loading was measured by ICP-AES on an IRIS Intrepid II XSP instrument (Thermo Electron Corporation). The morphologies of the materials were measured using a JSM-7800F SEM. The distribution of Pt nanoparticle size was determined using HAADF-STEM. The data were collected on the instrument of JEOL JEM-ARM200F. XPS measurement was performed using a ThermoFisher ESCALAB 250 Xi apparatus. The resulted binding energies needed to be calibrated by the value of carbon C 1s peak (284.6 eV). Prior to measurements, the sample was submitted to reduction at 200 °C by 20 vol% H_2/He.

2.3 Measurements of HCHO adsorption and oxidation

Both adsorption and oxidation process were finished in a fixed-bed microreactor with continuous flow, as shown in Figure 5, where the sample of 100 mg was filled in a U-type quartz tubular. The sample was flushed by helium for 30 min at 120 °C prior to performance test. As the temperature cooled to room temperature, the mixed feed gas of 300 ppm HCHO, 20 vol% O_2, He balance and 50% RH (relative humidity), was introduced into reactor. The condition of WHSV (weight hourly space velocity) equals to 30,000 mL h^{-1} g_{cat}^{-1}, conrresponding to the flow rate of 50 mL min^{-1}. HCHO was produced from passing helium through a container of paraformaldehyde in a thermostatic water bath with the concentration controlled by bath temperature and He flow rate. The RH value was tuned by varying the He flow rate.

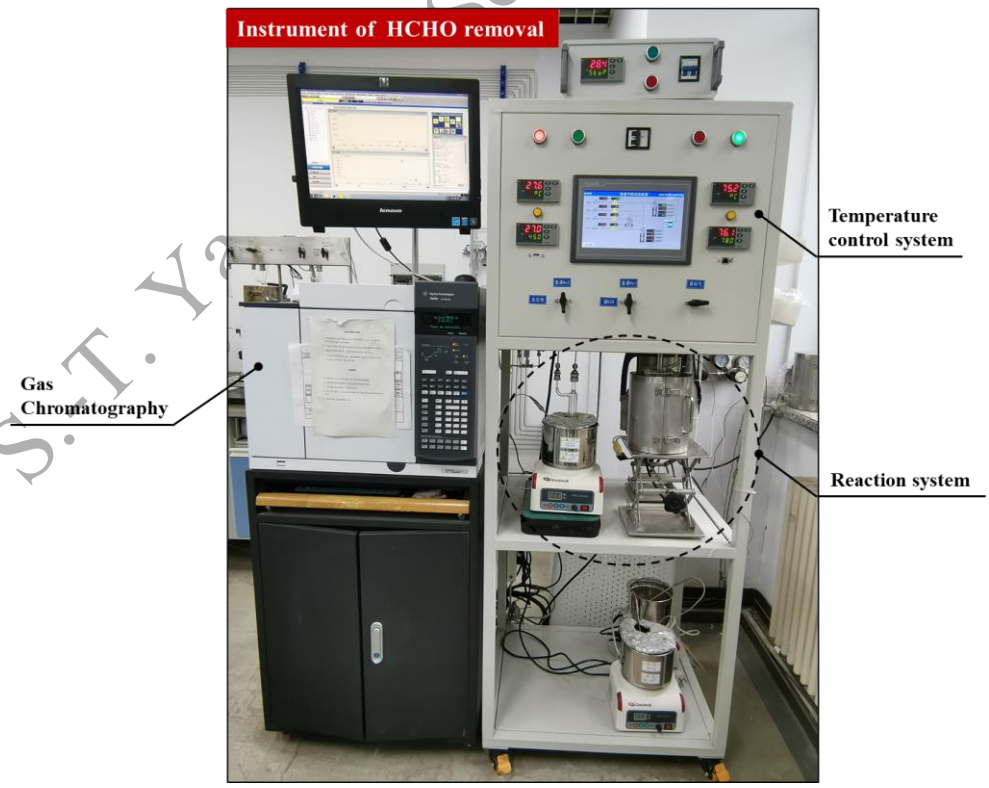

Figure 5. Images of fixed-bed instrument for HCHO adsorption and oxidation.

The concentration of HCHO or CO_2 is recorded by an on-line infrared spectrometer (Bruker MATRIX-MG01) in real-time. The storage capacities of HCHO were calculated according to Equation (1):

$$n_b = C_{HCHO}^{in} \cdot f \cdot t / m_{cat} \quad \text{Eq (1)}$$

Where C_{HCHO}^{in} represents the input concentration of HCHO with f: the total flow rate and t: breakthrough time that the outlet concentration of HCHO is less than 10% of the inlet HCHO concentration.). In addition, m_{cat} represents the amount of catalyst, of which the unit is grams.

The oxidation of HCHO on Pt/CAU-1-$(OH)_2$ was measured with the temperature rising. Before measurements, the catalysts were reduced by 20 vol % H_2/He at 200 °C. After reduction, the gas was swithced to helium, cooling to ambient temperature. The inputting gas (consisting of 180 ppm HCHO, 20 vol% O_2, 50% RH balanced with He) were introduced into the reaction tube. The room-temperature stability for catalytic oxidation was measured, as well. The gas chromatograph (GC Agilent 7890B) was employed to analyze the compositions of gases online. To obtain the equilibrium-conversion, the outlet gas was collected three times per hour at each temperature. Due to the low HCHO concentration, the FID (flame ionization detector) and a Ni catalysing convertor were equipped, with which the carbon oxides could be quantitatively transformed into methane. The conversion of HCHO was evaluated according to the following equation:

$$\alpha_{HCHO} = [CO_2]_{out}/[CO_2]_{feed} \times 100\ \% \quad \text{Eq (2)}$$

The HCHO conversion is expressed as α_{HCHO}, the concentration of produced CO_2 is written as $[CO_2]_{out}$ and the total concentration of CO_2 by the oxidation of all HCHO in the feedstock is marked as $[CO_2]_{feed}$.

3. RESULTS

3.1 Structural character and morphology

The XRD results of the as-synthesized CAU-1-$(OH)_2$ and CAU-1-NH_2 are displayed in Figure 6. Evidently, both the patterns are concided with the simulated XRD pattern and those previously published for these MOFs[14]. This result suggests that the pure CAU-1 MOFs are successfully synthesized. Following the loading of Pt nanoparticles, the sample of 0.1Pt/CAU-1-$(OH)_2$ still presents the typical peaks attributable to the CAU-1 X-ray diffraction profile and no pure platinum crystal phases. This implies that Pt nanoclusters have little impact on MOF structure. And the Pt species are in high dispersion which benefits from high surface area and rich hydroxyl groups to stabilize Pt nanoclusters.

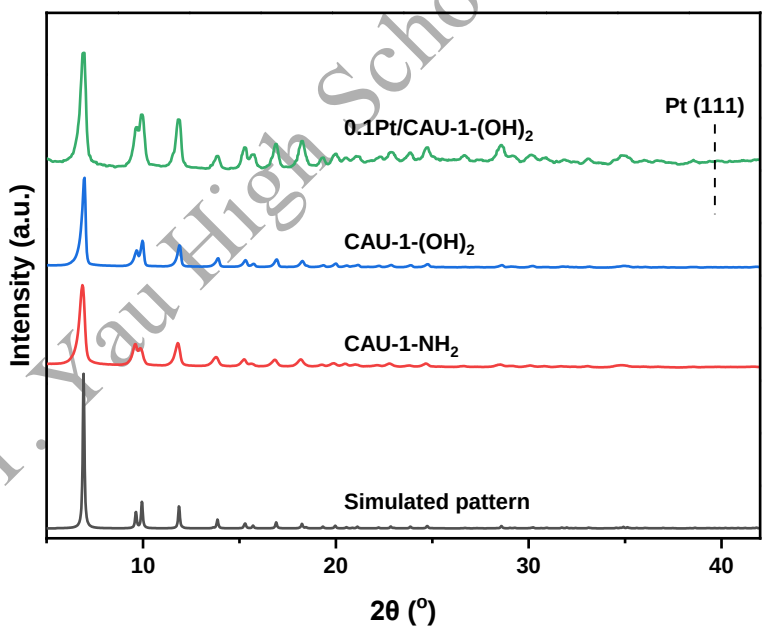

Figure 6. XRD patterns of CAU-1-NH_2, CAU-1-$(OH)_2$ and 0.1Pt/CAU-1-$(OH)_2$.

As presented in Figure 7, the N_2 adsorption-desorption isotherms of CAU-1-$(OH)_2$ and CAU-1-NH_2 display the shape of type-I with a high N_2 adsorption capacity, demonstrating the microporous structure of the bulk CAU-1 samples. The calculated surface area and pore volume

(at $P/P_0 = 0.95$) of CAU-1-$(OH)_2$ are 1296 $cm^2\ g^{-1}$ and 0.64 $cm^3\ g^{-1}$ (Table 1), respectively, in agreement with the previous values in literature[13]. The corresponding values for CAU-1-NH_2 are 1343 $cm^2\ g^{-1}$ and 0.63 $cm^3\ g^{-1}$. The large surface area and porous structure indicate high potential for HCHO adsorption. The thermal stabilities of CAU-1-$(OH)_2$ and CAU-1-NH_2 were investigated using thermogravimetric analysis. As shown in Figure 8, there is a slight initial mass loss at around 100 ºC that is typically associated with water adsorbed on the materials. The sharp peak emerging at ~300 °C is attributed to the decomposition of CAU-1, resulting in a complete collapse of the framework structure. That is, the structures of CAU-1-$(OH)_2$ and CAU-1-NH_2 could remain stable when the treatment temperature is below 300 °C. These results agree well with previous values published for these compounds, confirming successful synthesis of these MOFs.

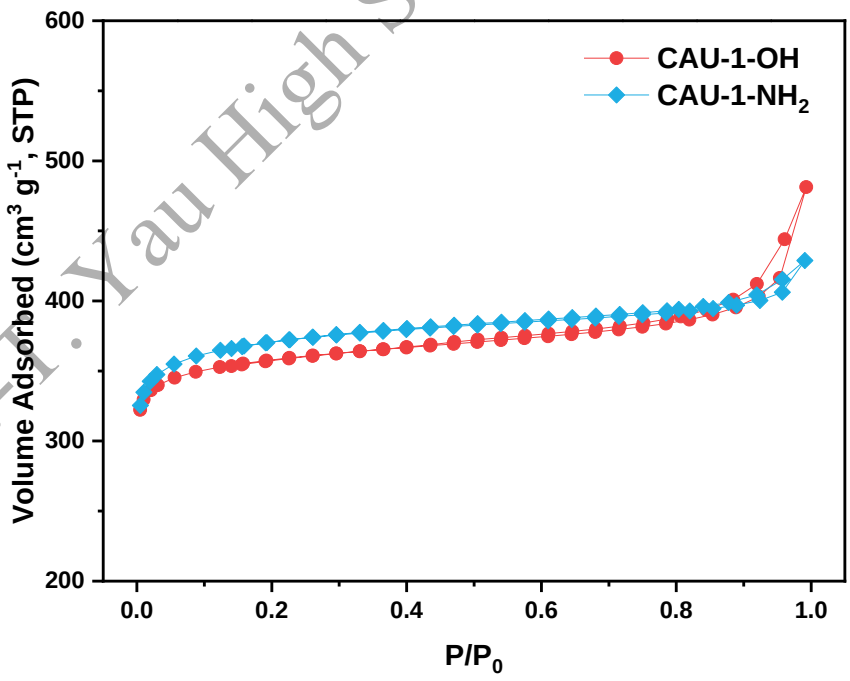

Figure 7. N_2 adsorption-desorption isotherms of CAU-1-$(OH)_2$ and CAU-1-NH_2.

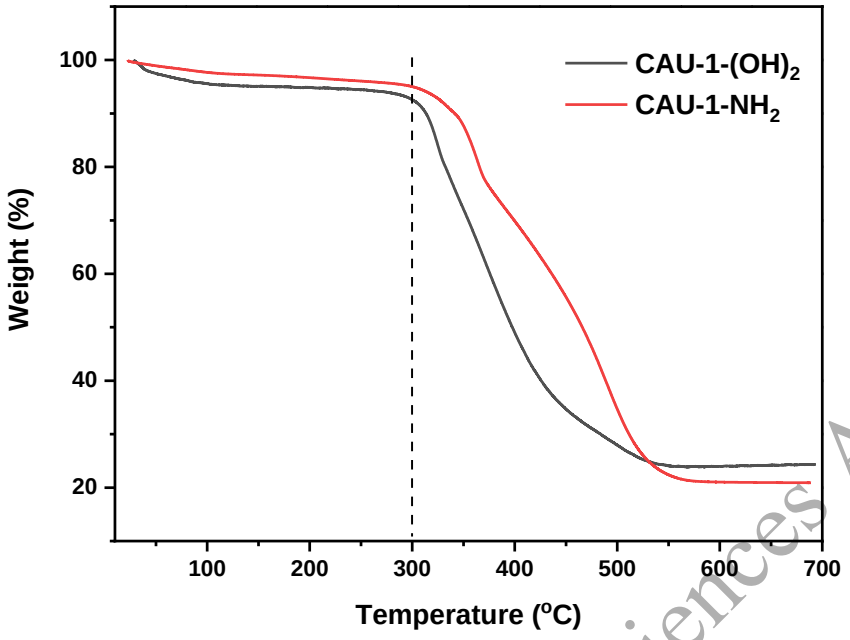

Figure 8. TG responses of the samples CAU-1-$(OH)_2$ and CAU-1-NH_2.

To visually observe morphology, SEM images with various magnifications were measured, as depicted in Figure 9. The as-synthesized CAU-1-$(OH)_2$ and CAU-1-NH_2, notably, exhibit different shapes. The particles of CAU-1-$(OH)_2$ (Figures 9a and b) possess the regular round-pie shape, while the short-rod shape for CAU-1-NH_2 (Figures 9c and d). Furthermore, the distribution of Pt nanoclusters was studied using the technology of HAADF-STEM. In Figure 10a, the Pt nanoclusters (the bright dots in the image) are uniformly dispersed on CAU-1-$(OH)_2$, resulting from the high surface area of CAU-1 and the abundance of hydroxyl groups to prevent Pt aggregation. Considering the particle size, around 200 particles were counted and the average size could be calculated as 1.1 nm. Additionally, Figure 10c depicts a HAADF-STEM image following usage of the material as a catalyst – the Pt remains similar dispersion with the calculated average size as 1.1 nm.

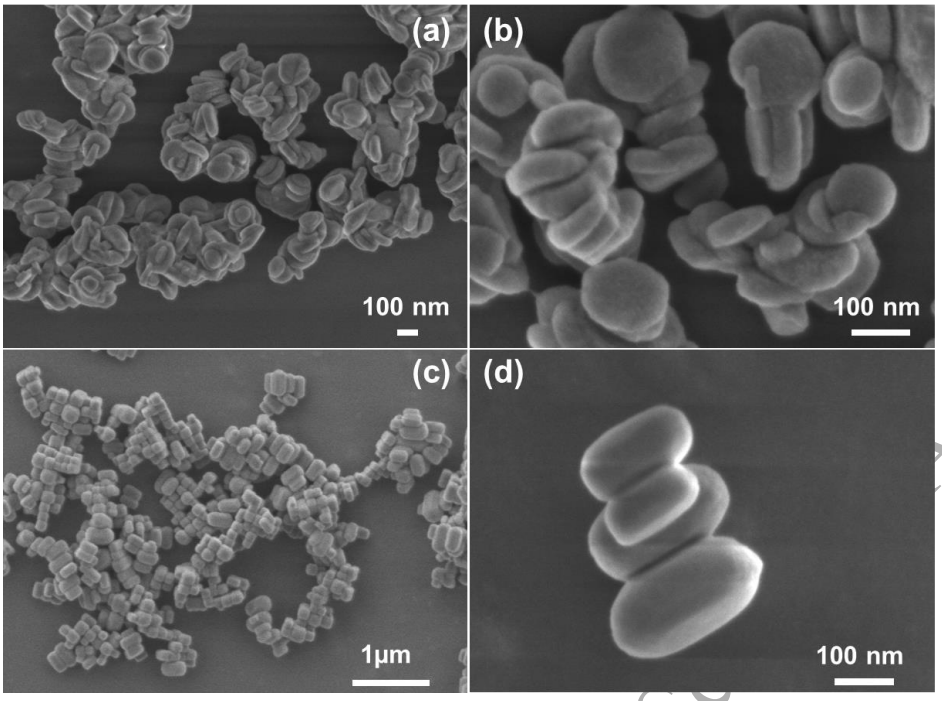

Figure 9. SEM images of (a,b) CAU-1-$(OH)_2$ and (c,d) CAU-1-NH_2.

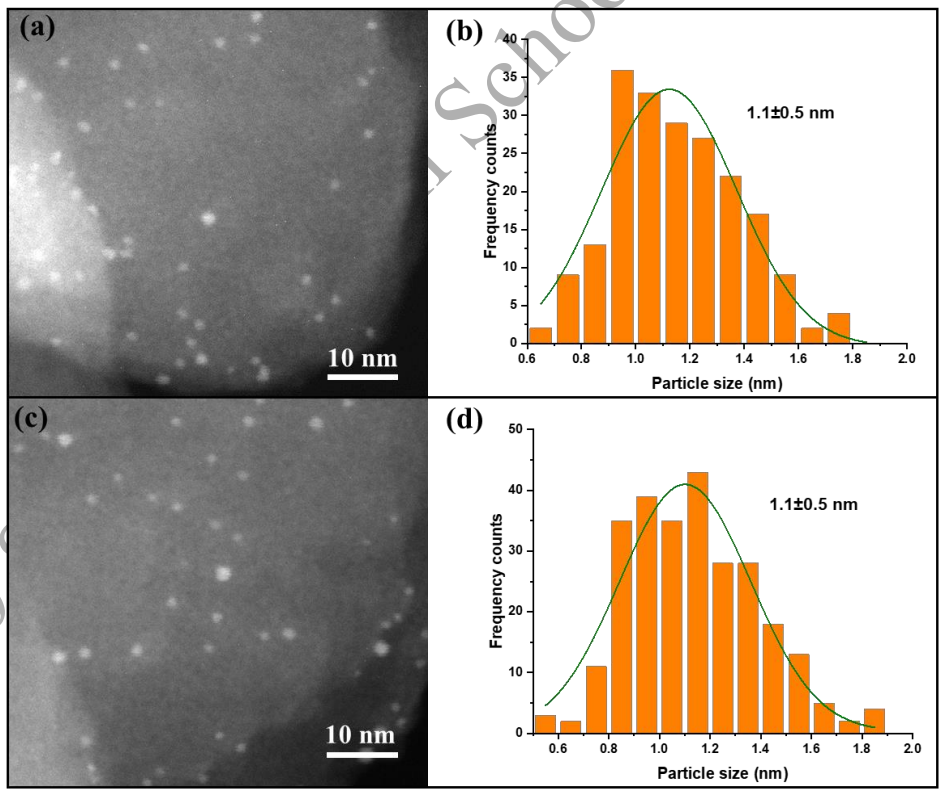

Figure 10. HAADF-STEM images of as-synthesized 0.1Pt/CAU-1-$(OH)_2$ (a,b) and used catalyst after stability test (c,d).

Another important parameter, valence state, of Pt nanoclusters in 0.1Pt/CAU-1-$(OH)_2$ is analyzed according to the XPS spectra of Pt 4f. As depicted in Figure 11, the peaks centered at 70.7 and 74.1 eV are assigned to Pt^0 species while the peaks at 71.7 and 75.1 eV correspond to the positive valence state of $Pt^{\delta+}$[16]. The ratio of $Pt^0/(Pt^0 + Pt^{\delta+})$ could be calculated to be 78%. This high content of Pt^0 is due to the fact that the precursor used in the preparation process is the metallic Pt^0 nanoclusters which was synthesized by the reduction of H_2PtCl_6 with EG[17].

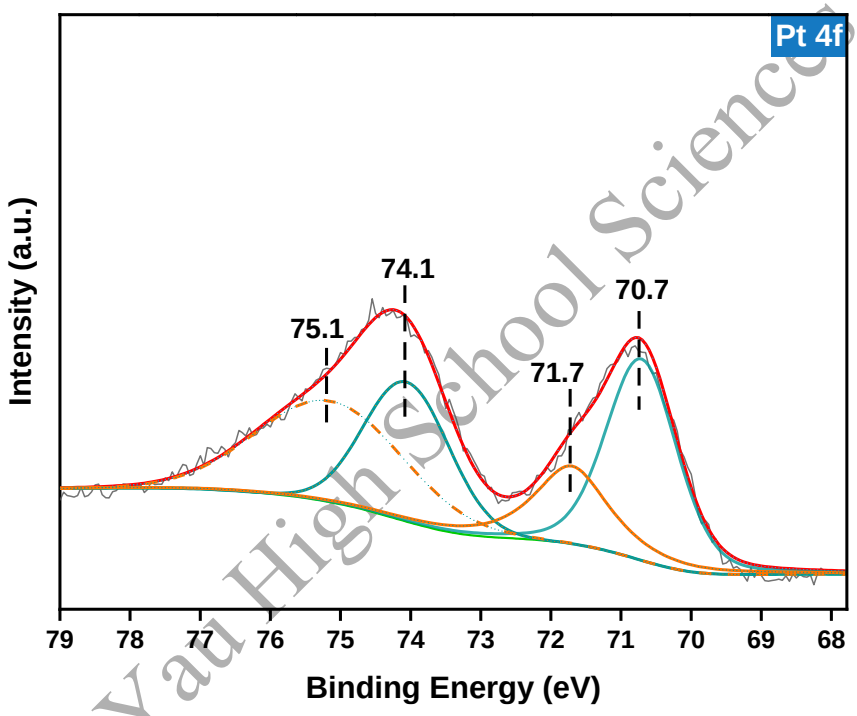

Figure 11. Pt 4f XPS spectra of 0.1Pt/CAU-1-$(OH)_2$.

3.2 Measurement of adsorption capacity

The dynamic curves of HCHO adsorption over the samples of CAU-1-$(OH)_2$ and CAU-1-NH_2 were recorded by infrared spectra to measure concentration in real-time. As displayed in Figure 12(a), the HCHO concentration decreases sharply when the feed gas is switched to CAU-1-$(OH)_2$; the outlet HCHO concentration then goes through a plateau near zero. Four hours later, the outlet concentration of HCHO rises above 10% of that of the feed gas, the

breakthrough time reaching. According to Eq (1), the evaluated value of HCHO capacity for CAU-1-$(OH)_2$ is as high as 1.6 mmol g_{cat}^{-1}. As would be expected, during the whole adsorption process, no CO_2 is detected in the outlet gas. This indicates the HCHO molecules are "stored" in the materials, wherein the HCHO is possibly transformed into the intermediate of formate with the help of hydroxyl groups[7]. For the other material of CAU-1-NH_2, as shown in Figure 12(b), a similar curve of HCHO concentration is obtained, but with a longer breakthrough time of around 8 h. Consequently, the adsorption capacity of HCHO for this material is a higher value of 3.2 mmol g_{cat}^{-1}. It has been previously proposed that in adsorbents (such as silicas and activated carbon) functionalized with amino groups, these groups can react with formaldehyde to form the imine (-N=CH_2)[4], resulting in an enhanced adsorption capacity for HCHO. Considering practical applications, only several ppm HCHO exists in the real environment; in such an environment, it can thus be deduced that the time of HCHO adsorption could be potentially extended to several months.

As illustrated in Table 1, the samples of CAU-1-$(OH)_2$ and CAU-1-NH_2 show significantly higher adsorption capacities than previously reported materials, such as activated carbon, Ag-MnO_x-CeO_2, CoMn etc.[9,10,18]. Thus, the as-synthesized materials of CAU-1-$(OH)_2$ and CAU-1-NH_2 exhibit remarkable advantages in terms of HCHO adsorption, imparting an outstanding potential in the role of catalyst support.

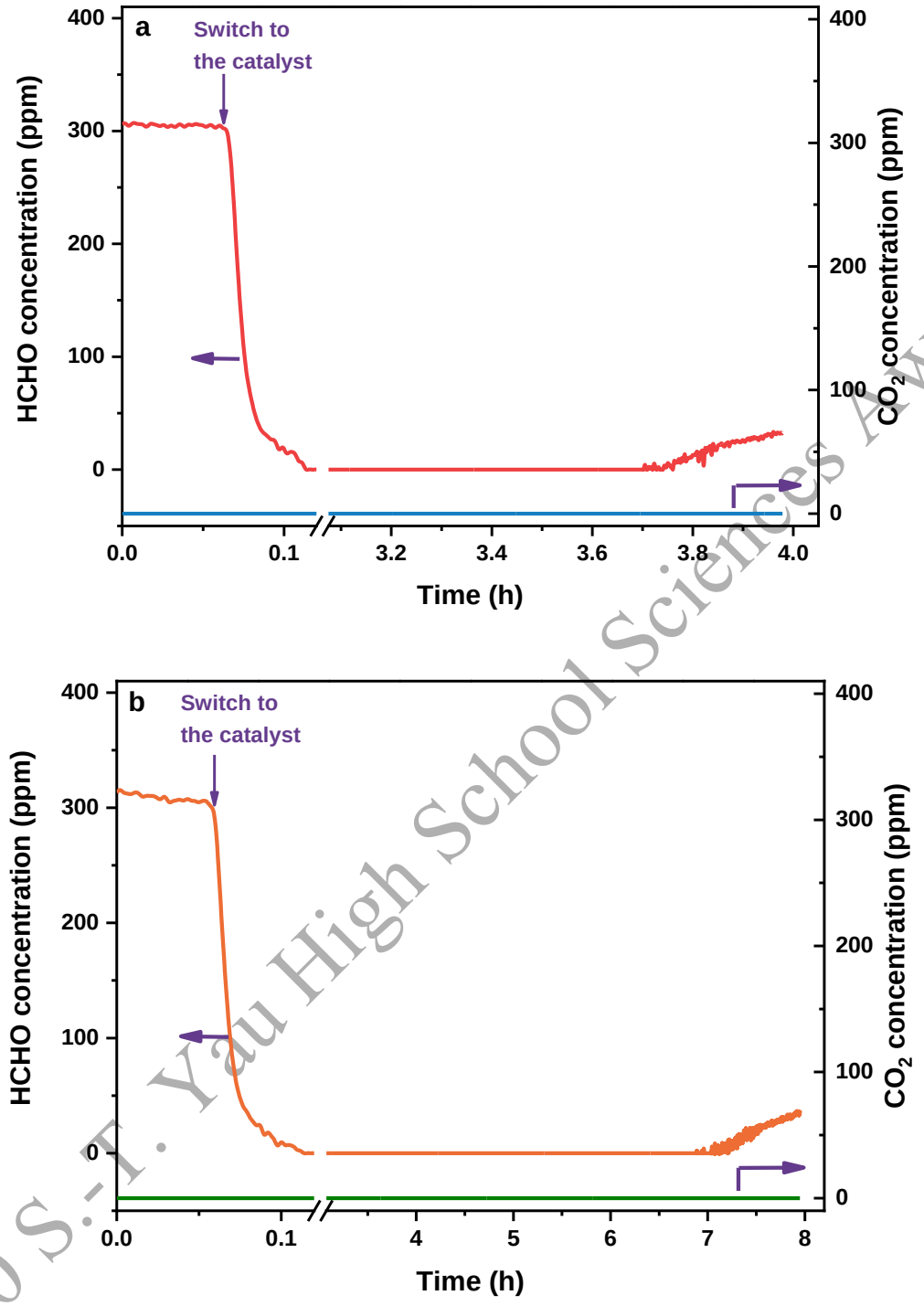

Figure 12. Real-time curves of HCHO and CO_2 concentrations during room-temperature HCHO adsorption on (a) CAU-1-$(OH)_2$ and (b) CAU-1-NH_2.

Table 1. Physical properties and the corresponding HCHO adsorption capacities of CAU type, compared with previously reported materials.

Sample	Pore volume ($cm^3\ g^{-1}$)	S_{BET} ($m^2\ g^{-1}$)	C_{HCHO} (ppm)	Reaction conditions	Storage capacity (mmol g_{cat}^{-1})	Ref
CAU-1-$(OH)_2$	0.64	1296	300	50 mL min^{-1}, T = 30 °C, RH = 50%	1.6	This work
CAU-1-NH_2	0.63	1343	300	50 mL min^{-1}, T = 30 °C, RH = 50%	3.2	This work
Activated carbon	0.49	1050	2.2	1.5 L min^{-1}, T = 25 °C, RH = 30%	0.13	Ma et al.[18]
Ag-MnO_x-CeO_2	0.31	102.2	80	100 mL min^{-1}, T = 20 °C, RH = 50%	0.43	Shi et al.[9]
CoMn	0.37	150	80	100 mL min^{-1}, T = 20 °C, RH = 50%	0.506	Wang et al.[10]

The catalytic activity of 0.1Pt/CAU-1-$(OH)_2$ was presented in Figure 13. When reactants of 300 ppm HCHO/20 vol% O_2/50% RH and helium balance are directed to the catalyst, the HCHO concentration rapidly drops to near zero at room temperature, while the product CO_2 concentration gradually increases. From the magnified figure of the inset in Figure 13, a delay of around 50 s occurs for the generation of CO_2 , following the initial fall in the HCHO concentration. It demonstrates that HCHO begin to remove by the storage. Later on, some of the stored HCHO is oxidized and released as the final products of CO_2 and H_2O; the 300 ppm HCHO is completely eliminated, but the outlet concentration of CO_2 is around 200 ppm. When the temperature rises to 40°C, more CO_2 is released due to the oxidation of the remaining stored HCHO. Therefore, HCHO is totally eliminated using the catalyst of 0.1Pt/CAU-1-$(OH)_2$ by the collaboration of adsorption and oxidation. For Pt/CAU-1-$(OH)_2$, two factors, the excellent

adsorption capacities of CAU-1 MOF and the oxidation ability of Pt, are indispensible.

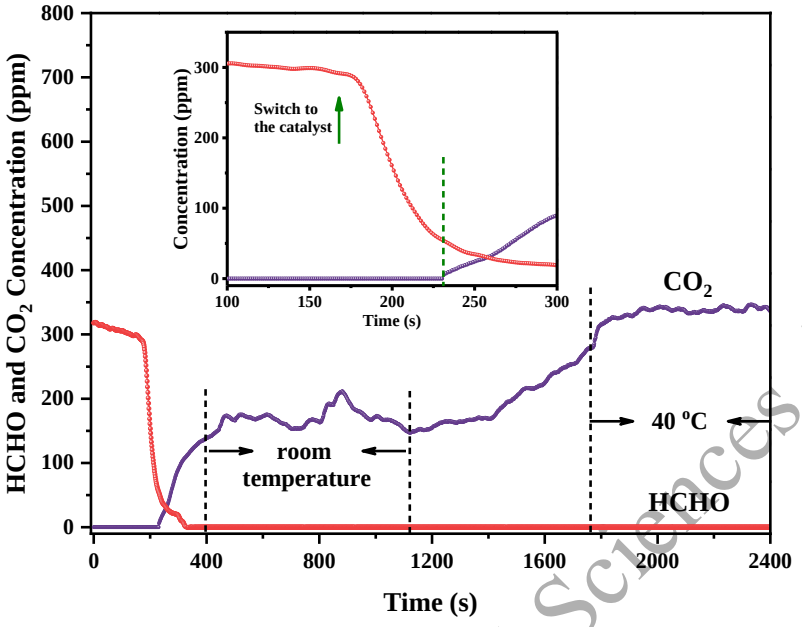

Figure 13. Real-time curves of HCHO and CO_2 concentrations during catalysis with 0.1Pt/CAU-1-$(OH)_2$. (Insert figure: magnification curves of the time range 100~300 s).

For comparison, γ-Al_2O_3 (aluminum oxide) played as a support to fabricate Pt/Al_2O_3 catalyst, and its HCHO removal capability was measured. As shown in Figure 14, when the feed gas switches to the catalyst at room temperature, the concentration of HCHO decreases from 300 to 77 ppm, and a concentration of 200 ppm CO_2 could be detected. Unfortunately, the HCHO could thus not be completely removed using the catalyst of Pt/Al_2O_3, which results from the limited capacity for storing the adsorbed HCHO on the support of Al_2O_3. Consequently, 0.1Pt/CAU-1-$(OH)_2$ herein possesses a better performance for HCHO elimination compared with traditional Pt/Al_2O_3, which demonstrates that the combination of adsorption and oxidation is more effective than the single oxidation step for the treatment of HCHO.

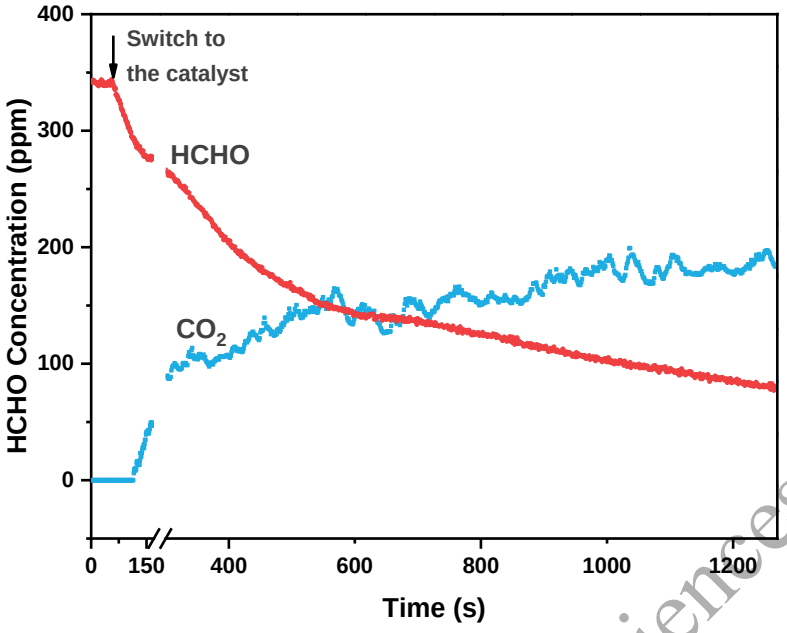

Figure 14. Real-time curves of HCHO and CO_2 concentrations during room-temperature HCHO adsorption on 0.05Pt/Al_2O_3 sample.

For further exploration of the oxidation activity, HCHO oxidation over Pt/CAU-1-$(OH)_2$ catalysts with different Pt loadings were measured. As shown in Figure 15, no conversion of HCHO is detected using just CAU-1-$(OH)_2$, consistent with the results of HCHO adsorption experiment. Around 67% HCHO conversion is obtained at 20 °C and a high value, 100% conversion, is achieved at 30 °C using 0.05Pt/CAU-1-$(OH)_2$. Further increasing Pt loading to 0.1 wt%, HCHO was 100% oxidized to CO_2 and H_2O at 20 °C using 0.1Pt/CAU-1-$(OH)_2$. Thus, although a lower loading would reduce the cost of the catalyst, this study suggests that 0.1 wt% is the optimal loading in terms of catalytic performance. The critical element for the high efficiency may be the Pt^0 nanoclusters. Furthermore, the stability is an indispensable element to be investigated as a catalyst regarding practical application. Figure 16 shows that 100% conversion of HCHO can be maintained for 36 h on the catalyst of 0.1Pt/CAU-1-$(OH)_2$ at room temperature. This maintenance of conversion suggests the retaining of catalyst structure

following reaction, Figure 10c and d, illustrating no aggregation with average size of 1.1 nm following use of catalyst.

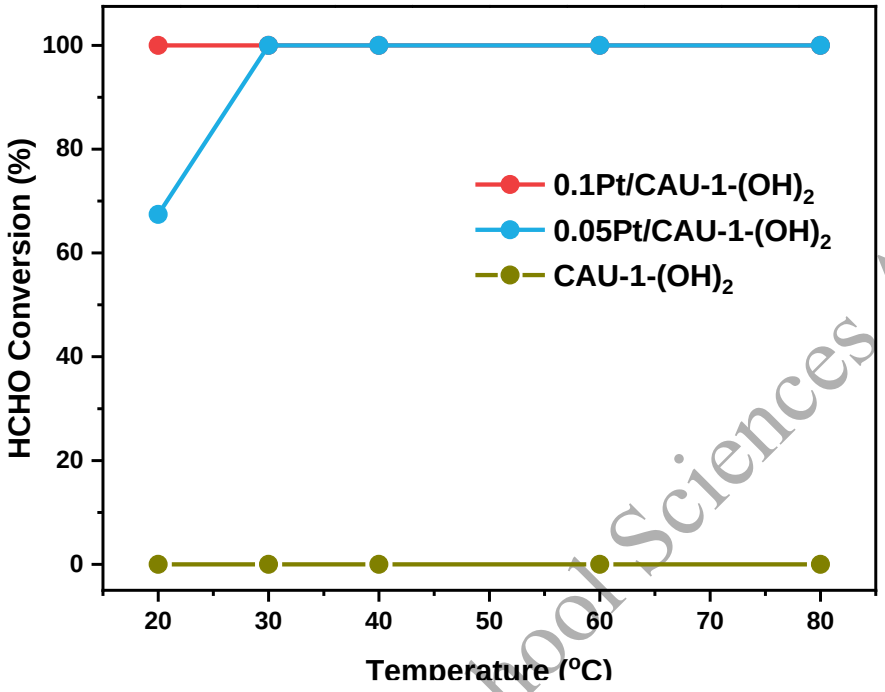

Figure 15. Curves of HCHO conversion with temperature over CAU-1-$(OH)_2$, 0.05Pt/CAU-1-$(OH)_2$ and 0.1Pt/CAU-1-$(OH)_2$.

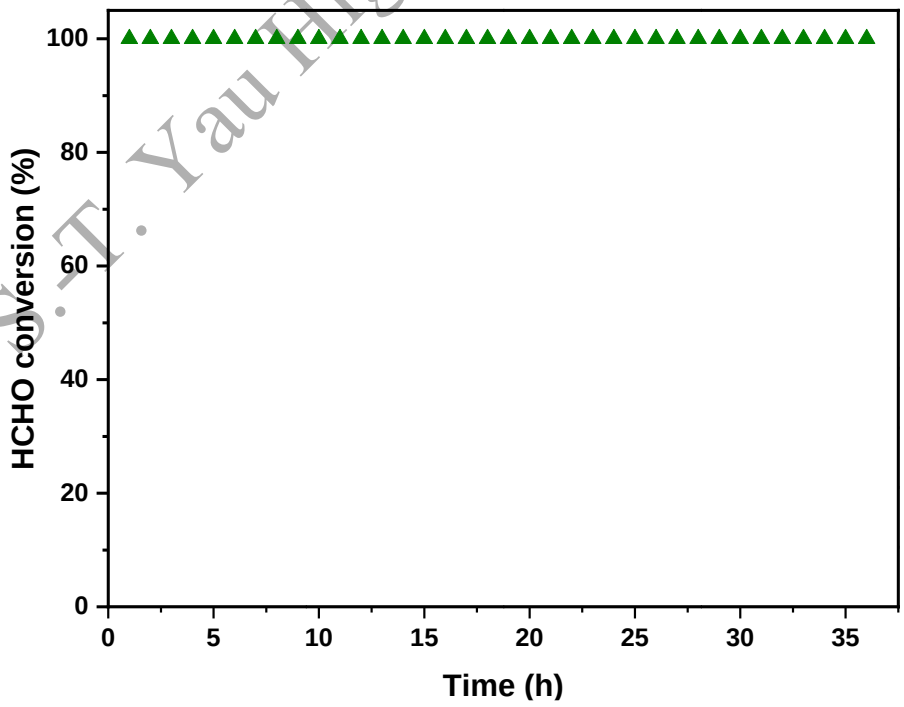

Figure 16. Stability of 0.1Pt/CAU-1-$(OH)_2$ at room temperature.

4. DISCUSSION

The collaborative method using adsorption and catalytic oxidation was identified as a potential approach to eliminate low concentration HCHO pollutant. MOF materials were chosen as the ideal candidates for the adsorbent and catalyst support for anchoring the noble metal particles due to their large surface areas, highly porous structures and modifiable function groups. In this work, the Al-based CAU MOF materials were employed to adsorb HCHO, and for the first time to support the active sites of Pt nanoclusters for HCHO oxidation. As for the HCHO adsorption capacity, both the MOFs CAU-1-NH_2 and CAU-1-$(OH)_2$ exhibit significantly higher values than previously reported adsorbents, as listed in Table 1. Besides the advantages from structure for adsorption, the functionalization with Lewis basic -NH_2 and -OH groups can also make contributions. In particular, the amino groups could react with the HCHO to form an imine (-N=CH_2, -NH_2 + HCHO → -N=CH_2 + H_2O), resulting in an adsorption capacity as high as 3.2 mmol g_{cat}^{-1} on CAU-1-NH_2[19]. The -OH groups could interact with the HCHO molecules via hydrogen bonding, facilitating conversion to formate intermediates (HCOO-, HCHO + -OH→ HCOO- + H_2O)[7], which are stored in the CAU-1-$(OH)_2$ at room temperature. After loading the 0.1 wt% Pt nanoclusters, the stored formate can be converted into CO_2 and H_2O, as shown in Figure 13. The complete elimination of 300 ppm HCHO using 0.1Pt/CAU-1-$(OH)_2$, compared with the much worse performance when using the conventional Pt/Al_2O_3, can be attributed to two important factors. One is the high adsorption capacity of CAU-1-$(OH)_2$, which leads to a prolonged adsorption lifetime. The other is the remarkable capability of this system for HCHO catalytic oxidation. Using 0.1Pt/CAU-1-$(OH)_2$, 180 ppm HCHO can be totally oxidized at 20 °C, as illustrated in Figure 15. This

performance is also superior to an alternative catalyst of Pt/ZrO_2 modified with a MOF, where the temperature required for total elimination of HCHO is over 70 °C even with a high Pt loading of 7 wt%, resulting in extra energy consumption for catalyst regeneration as well as high cost. For $0.1Pt/CAU\text{-}1\text{-}(OH)_2$, the remarkable performance in HCHO oxidation can give the credit to the uniform dispersion of Pt nanoclusters with size of 1.1 nm which is favorable for the O_2 activation. Thus, even with a much lowered Pt loading (0.1 wt%), the catalyst of $Pt/CAU\text{-}1\text{-}(OH)_2$ can realize complete oxidation at ambient conditions. In addition, good stability is presented by the catalyst of $Pt/CAU\text{-}1\text{-}(OH)_2$ which benefits from the stabilization of the uniformly dispersed Pt nanoclusters on the MOF.

The mechanism of HCHO removal via tandem adsorption and catalytic oxidation on $0.1Pt/CAU\text{-}1\text{-}(OH)_2$ can be summarized to occur via the process depicted in Figure 17. Firstly, HCHO adsorbs on the support of $CAU\text{-}1\text{-}(OH)_2$ and then transforms into formate species. Simultaneously, O_2 is split into activated oxygen atoms which can, then, decompose the formate into the non-toxic products of CO_2 and H_2O at ambient conditions. The process combing the adsorption and oxidation is realized by one-step on one specimen.

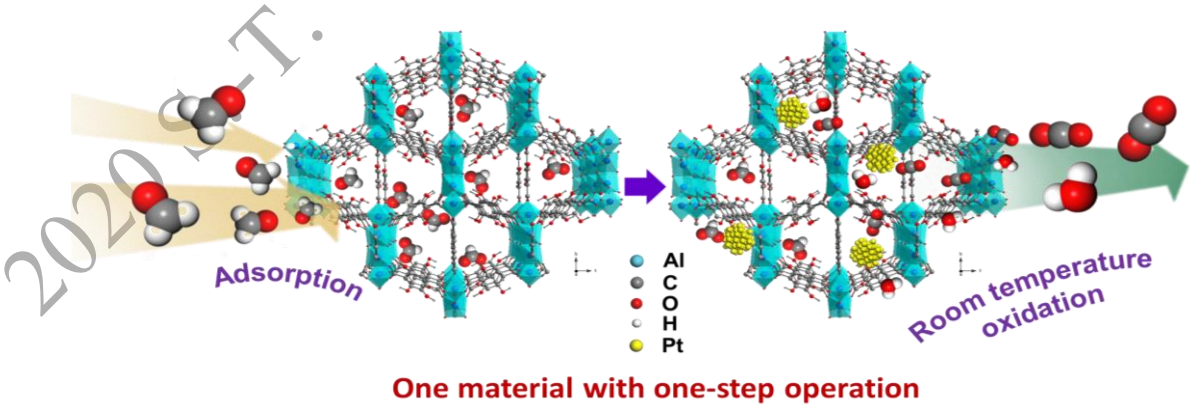

Figure 17. Schematic of HCHO elimination by tandem adsorption and catalytic oxidation on $Pt/CAU\text{-}1\text{-}(OH)_2$.

5. CONCLUSION

In summary, the Al-based metal-organic framework materials of CAU-1-$(OH)_2$ and CAU-1-NH_2 were fabricated. The large surface area, porous structure and Lewis basic hydroxyl/amino functional groups of these MOFs facilitate both the adsorption of HCHO, and the uniform Pt nanoclusters for the synthesis of a Pt/MOF catalyst. The adsorption capacities of HCHO measured on the CAU materials are much higher than previous materials. After loading with Pt nanoclusters, the stored formaldehyde is efficiently converted to CO_2 and H_2O on 0.1Pt/CAU-1-$(OH)_2$ at room temperature, due to the uniformly distributed Pt^0 nanoclusters. As a result, the whole elimination of HCHO is realized through a tandem mechanism by Pt/CAU-1 in one-step at room temperature. This strategy of developing a bifunctional catalyst that possesses high adsorption capacity and excellent oxidation ability could provide inspired guidance for methods to facilitate the elimination of other important atmospheric contaminants. Further future work can study on improving the catalyst that has been developed here – for instance, by attempting to utilize cheaper metals than platinum.

REFERENCES

[1] T. Salthammer, S. Mentese, R. Marutzky, Formaldehyde in the Indoor Environment[J], Chem. Rev., 110 (2010) 2536-2572.

[2] W. Ye, X. Zhang, J. Gao, G. Cao, X. Zhou, X. Su, Indoor air pollutants, ventilation rate determinants and potential control strategies in Chinese dwellings: A literature review[J], Sci. Total. Environ., 586 (2017) 696-729.

[3] J.P. Bellat, I. Bezverkhyy, G. Weber, S. Royer, R. Averlant, J.M. Giraudon, J.F. Lamonier, Capture of formaldehyde by adsorption on nanoporous materials[J], J. Hazard. Mater., 300 (2015) 711-717.

[4] C. Su, K. Liu, J. Zhu, H. Chen, H. Li, Z. Zeng, L. Li, Adsorption effect of nitrogen, sulfur or phosphorus surface functional group on formaldehyde at ambient temperature: Experiments associated with calculations[J], Chem. Eng. J., 393 (2020) 124729.

[5] J. Mo, Y. Zhang, Q. Xu, J.J. Lamson, R. Zhao, Photocatalytic purification of volatile organic compounds in indoor air: A literature review[J], Atmos. Environ., 43 (2009) 2229-2246.

[6] L.H. Nie, J.G. Yu, M. Jaroniec, F.F. Tao, Room-temperature catalytic oxidation of formaldehyde on catalysts[J], Catal. Sci. Technol., 6 (2016) 3649-3669.

[7] C.B. Zhang, F.D. Liu, Y.P. Zhai, H. Ariga, N. Yi, Y.C. Liu, K. Asakura, M. Flytzani-Stephanopoulos, H. He, Alkali-metal-promoted Pt/TiO2 opens a more efficient pathway to formaldehyde oxidation at ambient temperatures[J], Angew. Chem., Int. Ed., 51 (2012) 9628-9632.

[8] M. Guillemot, J. Mijoin, S. Mignard, P. Magnoux, Volatile organic compounds (VOCs) removal over dual functional adsorbent/catalyst system[J], Appl. Catal., B, 75 (2007) 249-255.

[9] C. Shi, B. Chen, X. Li, M. Crocker, Y. Wang, A. Zhu, Catalytic formaldehyde removal by ‘‘storage-oxidation’’ cycling process over supported silver catalysts[J], Chem. Eng. J., 200-202 (2012) 729-737.

[10] Y. Wang, A. Zhu, B. Chen, M. Crocker, C. Shi, Three-dimensional ordered mesoporous Co-Mn oxide: A highly active catalyst for “storage-oxidation” cycling for the removal of formaldehyde[J], Catal. Commun., 36 (2013) 52-57.

[11] S. Kumar, S. Jain, M. Nehra, N. Dilbaghi, G. Marrazza, K.H. Kim, Green synthesis of metal-organic frameworks: A state-of-the-art review of potential environmental and medical applications[J], Coord. Chem. Rev., 420 (2020) 213407-213435.

[12] X. Zheng, S. Liu, S. Rehman, Z. Li, P. Zhang, Highly improved adsorption performance of metal-organic frameworks CAU-1 for trace toluene in humid air via sequential internal and external surface

modification[J], Chem. Eng. J., 389 (2020) 123424-123432.

[13] X. Si, C. Jiao, F. Li, J. Zhang, S. Wang, S. Liu, Z. Li, L. Sun, F. Xu, Z. Gabelica, C. Schick, High and selective CO_2 uptake, H_2 storage and methanol sensing on the amine-decorated 12-connected MOF CAU-1[J], Energy Environ. Sci., 4 (2011) 4522-4527.

[14] T. Ahnfeldt, N. Guillou, D. Gunzelmann, I. Margiolaki, T. Loiseau, G. Ferey, J. Senker, N. Stock, $[Al_4(OH)_2(OCH_3)_4(H_2N\text{-}BDC)_3]$. xH_2O: a 12-connected porous metal-organic framework with an unprecedented aluminum-containing brick[J], Angew. Chem. Int. Ed., 48 (2009) 5163-5166.

[15] N. An, S. Li, P.N. Duchesne, P. Wu, W. Zhang, J.-F. Lee, S. Cheng, P. Zhang, M. Jia, W. Zhang, Size Effects of Platinum Colloid Particles on the Structure and CO Oxidation Properties of Supported Pt/Fe2O3Catalysts[J], J. Phys. Chem. C, 117 (2013) 21254-21262.

[16] L. Li, L. Li, L. Wang, X. Zhao, Z. Hua, Y. Chen, X. Li, X. Gu, Enhanced catalytic decomposition of formaldehyde in low temperature and dry environment over silicate-decorated titania supported sodium-stabilized platinum catalyst[J], Appl. Catal., B, 277 (2020) 119216.

[17] J. Quinson, M. Inaba, S. Neumann, A.A. Swane, J. Bucher, S.B. Simonsen, L. Theil Kuhn, J.J.K. Kirkensgaard, K.M.Ø. Jensen, M. Oezaslan, S. Kunz, M. Arenz, Investigating Particle Size Effects in Catalysis by Applying a Size-Controlled and Surfactant-Free Synthesis of Colloidal Nanoparticles in Alkaline Ethylene Glycol: Case Study of the Oxygen Reduction Reaction on Pt[J], ACS Catal., 8 (2018) 6627-6635.

[18] C. Ma, X. Li, T. Zhu, Removal of low-concentration formaldehyde in air by adsorption on activated carbon modified by hexamethylene diamine[J], Carbon, 49 (2011) 2873-2875.

[19] D.I. Kim, J.H. Park, S.D. Kim, J.Y. Lee, J.-H. Yim, J.-K. Jeon, S.H. Park, Y.K. Park, Comparison of removal ability of indoor formaldehyde over different materials functionalized with various amine groups[J], J. Ind. Eng. Chem., 17 (2011) 1-5.

ACKNOWLEDGEMENT

When I participated in the Science Public Day of Dalian Institute of Chemical Physics (DICP) in 2017, I learned from the scientific report of Prof. Jian Lin that more and more people suffer from Sick-Building-Syndrome (SBS) for the ever-increasing amount of time that we spend indoors. Specifically, formaldehyde is dominant pollutant indoor which can exert a detrimental effect on human health. In daily life, I noticed that an air purifier has become necessary in many households. However, the filter element needs to be replaced regularly due to its limited adsorption capacity. This problem aroused my interest to study the HCHO removal. Immediately, I contacted Prof. Jian Lin and consulted him on the issues of indoor air purification. He is enthusiastic about science-education among teenagers. And I am very glad to go to his lab to carry out the experiments at weekends and leisure time. I sincerely promised him that I would protect myself in the experiment process and take the expenses by myself. Under his guidance, I read some professional references and learned many experimental technologies including the preparation of catalyst, catalytic activity evaluation and the corresponding characterizations. With a deep understanding, I got that the method of combining the adsorption and catalytic oxidation is a potential to realize practical use in HCHO removal. Previously, I have also read about the growing applications of MOFs, and was intrigued by the potential to apply them in this situation. Together, myself and Prof. Jian Lin conceived a plan for this project and I then conducted the experiments to accomplish this report.

I greatly thank my supervisor Prof. Jian Lin for his provision of the experimental facilities in DICP, his patient guidance and helpful discussions of the experiments. I am also grateful for his valuable advice on the organization and writing of this report. I also express my gratitude

to Prof. Lin Li, skilled and experienced concerning characterization technique for catalysis and adsorption studies, for assisting me with the characterizations, such as SEM, STEM, TG, XRD and XPS. And Thanks for Dr. Xiucheng Sun's help in experimental operation.

Finally, I wish to thank my parents for their encouragement and financial assistance.

RESUME

Resume of Team Member

Name: Yuehan Wang

Email: yuwang@student.oakschristian.org

Education

High school: Oaks Christian School, 31749 La Tienda Drive, Westlake Village, CA 91362

Standard GPA 4.0, Weighted GPA 4.42 (top 5%)

TOEFL 110, test date: June 25, 2020 (Reading 30, Listening 28, Speaking 24, Writing 28)

Middle school: Dalian No.9 Middle School, China

Leadership Experience

Oaks Christian School Chemistry Club Vice President

Publications

[1] X.C. Sun, J. Lin, H.L. Guan, L. Li, L. Sun, **Y.H. Wang**, S. Miao, Y. Su, X.D. Wang, Complete oxidation of formaldehyde over TiO_2 supported subnanometer Rh catalyst at ambient temperature, Appl. Catal., B, 226 (2018) 575-584.

[2] X.C. Sun, J. Lin, Y. Chen, **Y.H. Wang**, L. Li, S. Miao, X.L. Pan, X.D. Wang, Unravelling platinum nanoclusters as active sites to lower the catalyst loading for formaldehyde oxidation, Commun. Chem., 2 (2019) 27-37.

[3] X.C. Sun, J. Lin, **Y.H. Wang**, L. Li, X.L. Pan, Y. Su, X.D. Wang, Catalytically active Ir^0 species supported on Al_2O_3 for complete oxidation of formaldehyde at ambient temperature, Appl. Catal., B, 268 (2020) 118741-118750.

Resume of the supervisor

Prof. Jian Lin (Email: jianlin@dicp.ac.cn)

Jian Lin is a full professor and master supervisor at Dalian Institute of Chemical Physics and a member of Youth Innovation Promotion Association. His research areas focus on the development of subnanometer and single atom catalysts for applications in air purification, ethane dehydrogenation and hydrogen energy related catalysis processes. He has published more than 40 papers in journals specializing in catalysis and chemical engineering, such as Angewandte Chemie International Edition, Applied Catalysis B: Environmental et al.

Prof. Lin Li (Email: llin@dicp.ac.cn)

Prof. Lin Li received his PhD degree from Dalian Institute of Chemical Physics in 2006. His research interests include the development and application of *in situ* characterization techniques for catalysis research, such as *in situ*/operando FT-IR and adsorption microcalorimetry, and he received the honor of Key Technical Personnel of Chinese Academy of Sciences in 2018.

本参赛团队声明所提交的论文是在指导老师指导下进行的研究工作和取得的研究成果。尽本团队所知，除了文中特别加以标注和致谢中所罗列的内容以外，论文中不包含其他人已经发表或撰写过的研究成果。若有不实之处，本人愿意承担一切相关责任。

参赛队员：王珂涵　　指导老师：林堂

李林

2020 年 09 月 13 日